Coulomb dissociation of O-16 into He-4 and C-12

N.B. When citing this work, cite the original published paper.

(article starts on next page)

Coulomb dissociation of ^{16}O into ^{4}He and ^{12}C

Lukas Thomas Bott[1,*], *Kathrin* Göbel[2,1], *Michael* Heil[3], *Aleksandra* Kelić-Heil[3], *René* Reifarth[1], *Marialuisa* Aliotta[1,4], *Tahani* Almusidi[5,6], *Hector* Alvarez-Pol[7], *Leyla* Atar[8], *Liam* Atkins[5], *Thomas* Aumann[8,3], *Daniel* Bemmerer[9], *José* Benlliure[7], *Carlos* Bertulani[10], *Konstanze* Boretzky[3], *Benjamin* Brückner[1], *Leonhard* Brandenburg[1], *Giovanni* Bruni[23], *Pablo* Cabanelas Eiras[7], *Christoph* Caesar[3], *Enrique* Casarejos[11], *Joakim* Cederkall[12], *Leonid* Chulkov[13], *Dolores* Cortina-Gil[7], *Andrey* Danilov[13], *Enrico* De Filippo[14], *Sophia Florence* Dellmann[1], *Isabell* Deuter[1], *José Antonio* Dueñas Díaz[15], *Meytal* Duer[8], *Zoltan* Elekes[16], *Philipp* Erbacher[1], *Sonia* Escribano Rodriguez[5], *Zsolt* Fülöp[16], *Ashton* Falduto[8], *Manuel* Feijoo[7], *Stefan* Fiebiger[1], *Igor* Gašparić[17], *Daniel* Galaviz[18], *María José* García Borge[19], *Gabriel* García-Jiménez[7], *Elena* Geraci[20], *Roman* Gernhäuser[21], *Jan* Glorius[3], *Brunilde* Gnoffo[20], *David* González Caamaño[7], *Antia* Graña González[7], *Alexander* Grein[1], *Anna-Lena* Hartig[8], *Tanja* Heftrich[1], *Henning* Heggen[3], *Marcel* Heine[22], *Andreas* Heinz[23], *Corinna* Henrich[8], *Thomas* Hensel[9,24], *Matthias* Holl[8,23], *Ilja* Homm[8], *Ákos* Horváth[25], *Andrea* Horvat[8], *Andrea* Jedele[8], *Desa* Jelavic Malenica[8], *Tobias* Jenegger[21], *Håkan T.* Johansson[23], *Björn* Jonson[23], *Julian* Kahlbow[8], *Nasser* Kalantar-Nayestanaki[26], *Armel* Kamenyero[27], *Kafa* Khasawneh[1], *Oleg* Kiselev[3], *Philipp* Klenze[21], *Marco* Knösel[8], *Karsten* Koch[3], *Marvin* Kohls[1], *Daniel* Körper[3], *Thorsten* Kröll[8], *Sabina* Krasilovskaja[1], *Dmytro* Kresan[3], *Deniz* Kurtulgil[1], *Nikolaus* Kurz[3], *Bastian* Löher[3], *Christoph* Langer[1,28], *Claudia* Lederer-Woods[4], *Christopher* Lehr[8], *Yuri A* Litvinov[3], *Enis* Lorenz[8], *Nunzia Simona* Martorana[29], *Tohru* Motobayashi[30], *Silvia* Murillo Morales[5], *Enrique* Nacher[31], *Thomas* Nilsson[23], *Emanuele Vincenzo* Pagano[29], *Valerii* Panin[3], *Joochun* Park[12,32], *Stefanos* Paschalis[5], *Angel* Perea[19], *Marina* Petri[5], *Sara* Pirrone[14], *Ralf* Plag[3], *Lukas* Ponnath[21], *Romana* Popočovski[17], *Markus* Reich[1], *Han-Bum* Rhee[8], *Jose Luis* Rodriguez Sanchez[7], *Dominic* Rossi[3,8], *Paolo* Russotto[29], *Ángel-Miguel* Sánchez-Benítez[15], *Christian* Sürder[8], *Deniz* Savran[3], *Heiko* Scheit[8], *Konrad* Schmidt[9], *Hendrik* Schulte[1], *Haik* Simon[3], *Johannes* Simon[8], *Viktor* Starostin[13], *Sonja* Storck-Dutine[8], *Hans Toshihide* Törnqvist[3,8], *Junki* Tanaka[8], *Olof* Tengblad[19], *Benedikt* Thomas[1], *Marina* Trimarchi[14,33], *Stefan* Typel[8,3], *László* Varga[3], *Klaus* Volk[1], *Meiko* Volknandt[1], *Vadim* Wagner[8], *Felix* Wamers[3], *Mario* Weigand[1], and *Lorenzo* Zanetti[8]

[1]Goethe Universität Frankfurt, Germany

[2]Facility for Antiproton and Ion Research in Europe GmbH, Germany

[3]GSI Helmholtzzentrum für Schwerionenforschung Darmstadt, Germany

[4]University of Edinburgh, United Kingdom

[5]University of York, United Kingdom

[6]King Saud University, Saudi Arabia

[7]University of Santiago de Compostela, Spain

[8]Technische Universität Darmstadt, Germany

[9]Helmholtz-Zentrum Dresden-Rossendorf, Germany

[10]Texas A&M University-Commerce, USA

[11]CINTECX, Universidade de Vigo, Spain

[12]Lund University, Sweden

*e-mail: bott@iap.uni-frankfurt.de

[13]NRC Kurchatov Institute Moscow, Russia

[14]INFN-Sezione di Catania, Italy

[15]Universidad de Huelva, Spain

[16]ATOMKI Debrecen, Hungary

[17]Ruđer Bošković Institute, Zagreb, Croatia

[18]University of Lisboa, Portugal

[19]CSIC Madrid, Spain

[20]Università di Catania, Italy

[21]Technische Universität München, Germany

[22]Institut Pluridisciplinaire Hubert CURIEN, France

[23]Chalmers University of Technology, Sweden

[24]Technische Universität Dresden, Germany

[25]Eötvös Loránd University, Hungary

[26]ESRIG, University of Groningen, The Netherlands

[27]GANIL, France

[28]University of Applied Science Aachen, Germany

[29]INFN Laboratori Nazionali del Sud, Italy

[30]RIKEN, Nishina Center for Accelerator-Based Science, Japan

[31]IFIC, CSIC-Universidad de Valencia, Spain

[32]Center for Exotic Nuclear Studies, Institute for Basic Science, Republic of Korea

[33]Università degli Studi di Messina, Italy

Abstract. We measured the Coulomb dissociation of ^{16}O into ^{4}He and ^{12}C within the FAIR Phase-0 program at GSI Helmholtzzentrum für Schwerionenforschung Darmstadt, Germany. From this we will extract the photon dissociation cross section ^{16}O$(\alpha,\gamma)^{12}$C, which is the time reversed reaction to ^{12}C$(\alpha,\gamma)^{16}$O. With this indirect method, we aim to improve on the accuracy of the experimental data at lower energies than measured so far.

The expected low cross section for the Coulomb dissociation reaction and close magnetic rigidity of beam and fragments demand a high precision measurement. Hence, new detector systems were built and radical changes to the R^{3}B setup were necessary to cope with the high-intensity ^{16}O beam. All tracking detectors were designed to let the unreacted ^{16}O ions pass, while detecting the ^{12}C and ^{4}He.

1 The ^{12}C$(\alpha,\gamma)^{16}$O fusion reaction

During their evolution stars will undergo several burning phases and reach eventually the so called triple-alpha process where three ^{4}He nuclei are fused into carbon. At the same time several other processes may take place, whereby the fusion of carbon and helium into oxygen is of particular interest. DeBoer [1] and Aliotta [2] give an excellent overview of the recent developments. The ^{12}C$(\alpha,\gamma)^{16}$O fusion reaction determines the carbon-to-oxygen ratio at the end of the helium burning phase and, hence, the further evolution and fate of the star. Furthermore, this reaction is also crucial for the carbon-to-oxygen ratio in the universe and thus for the creation of the essential elements for life as we know it on earth.

The fate of stars in the mass range between about 14 M$_{\odot}$ and 60 M$_{\odot}$ is still unknown because of the uncertainty of the ^{12}C$(\alpha,\gamma)^{16}$O reaction [3, 4]. To generate reliable nucleosynthesis simulations for these astrophysical purposes, the reaction rate of ^{12}C$(\alpha,\gamma)^{16}$O in the astrophysical relevant energy region around 300 keV has to be known with uncertainties of less than 10%.

Theoretical calculations and extrapolation from higher energies result in an extremely low value of about 10^{-17} b, which poses a significant challenge for direct measurements. Available experimental data down to 1 MeV show sometimes large uncertainties of up to 100% [1].

With their larger cross sections indirect measurements promise to improve the experimental data quality in the low center-of-mass energy region.

2 Coulomb dissociation of ^{16}O at R^{3}B

In order to determine the ^{12}C$(\alpha,\gamma)^{16}$O fusion reaction, there are different experimental approaches available, see e.g. [5, 6]. The indirect method of Coulomb dissociation of ^{16}O is particularly promising and can bridge the gap to the stellar energy regime. Baur, Bertulani and Rebel proposed this measurement in 1986 [7] for the first time and performed detailed calculations later [8, 9]. The Coulomb dissociation cross section is far larger than the direct measurement and profits from the large number of virtual photons if it is performed at relativistic energies.

We measured the Coulomb dissociation of ^{16}O into ^{4}He and ^{12}C in inverse kinematics at the R^{3}B setup, within the FAIR Phase-0 campaign at GSI Helmholtzzentrum für Schwerionenforschung in Darmstadt Germany. A high-intensity ^{16}O beam impinged on a selection of different targets. In the Coulomb field of the target nuclei the ion can be excited and eventually break up into ^{4}He and ^{12}C. At beam energies of 300 MeV/nucleon, using a lead target of 80 mg/cm^2, and an ^{16}O beam of $2 \cdot 10^9$ ions per second we estimated a count rate of 30 counts per day at a center-of-mass energy of E_{cm} = 1 MeV. With the recorded data in the energy range of 800 keV to 5 MeV we expect a significant reduction of statistic uncertainties compared to the available data. Typical systematic uncertainties of Coulomb dissociation measurements in the past were about 10% to 15%. However the systematic uncertainties in our case will be small since we can use the well measured resonances at higher energies for an absolute normalization.

A low Z target like carbon contributes mainly to the nuclear breakup reaction. By subtracting the nuclear contribution from breakup reactions occurring in the lead target we are able to extract the desired Coulomb dissociation reaction cross section. Possible interference effects can be studied by using an intermediate mass target like Sn [10].

2.1 The setup

The magnetic rigidity of the unreacted ^{16}O beam and the fragments ^{12}C and ^{4}He are close since the mass-to-charge-number ratio A/Z = 2. The scintillation detectors can measure intensities of up to 10^6 ions per second. To allow the high-intensity unreacted beam to pass the tracking detectors and measure both fragments, radical changes to the R^{3}B setup [11, 12] were necessary. All detectors where designed and positioned so as to let the unreacted ions pass.

Figure 1 shows a sketch of the modified R^{3}B setup. All detectors relevant for tracking, charge identification and intensity measurement are positioned inside a vacuum chamber connected to each other. This allows a direct connection to the accelerator without the use of windows which would drastically increase unwanted reactions with the beam. Two active collimators, ROLU (Rechts-Oben-Links-Unten), in front of the target cut the beam dimension by creating a veto. During the beam setup phase they helped to center the ^{16}O beam on the target. Around the target the CALIFA (CALorimeter for In-Flight detection of gamme-rays and high energy charged pArticles) calorimeter measures γ-rays from excited fragments.
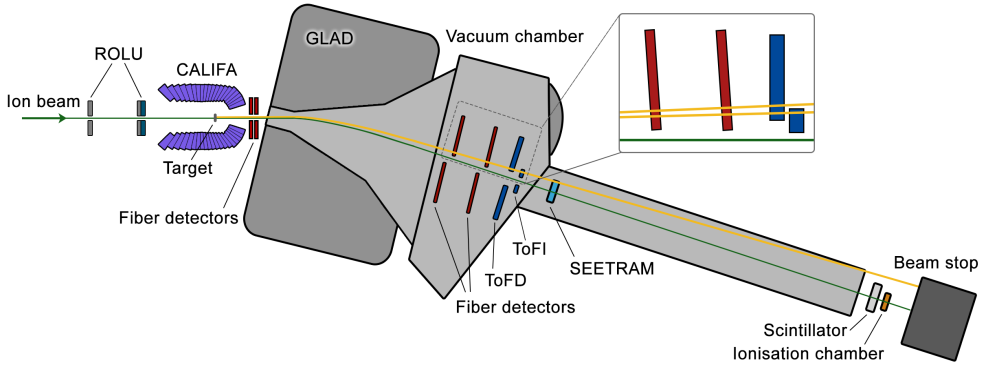
Figure 1. Sketch of the experimental setup at R^{3}B as it was used for the Coulomb dissociation of ^{16}O. Two active collimators, ROLU, in front of the target cut the beam dimension by creating a veto focus and help to center the ion beam on the target. γ-rays from excited ^{12}C are measured in the CALIFA calorimeter. For tracking of the fragments two fiber detectors in front of the magnet GLAD measure the x- and y-position. Two pairs of fiber detectors downstream from GLAD measure the x-position. The time-of-flight walls ToFD and ToFI allow to extract the charge of the fragments, based on their energy loss. All tracking detectors had slits or a hole and were mounted on drives to allow the unreacted beam to pass without damaging the detectors or causing high dead time by its high intensity. A secondary electron transmission monitor (SEETRAM) detector as well as a scintillator and an ionization chamber measured the beam intensity.

In front of the superconducting magnet GLAD (GSI Large Acceptance Dipole) a pair of 250 μm thick 10x10 cm^2 organic fiber scintillators measures the x- and y-positions of the fragments. Mounted on x/y drives a 3 mm diameter hole can be adjusted to let the unreacted ^{16}O beam pass. The x-position of the deflected fragments are measured with 1000 μm thick 50x50 cm^2 fiber scintillators positioned behind GLAD in two pairs. These detectors are mounted on x-drives to adjust the gap. A small rotation about the y-axis increases their detection efficiency and each fiber is read out by two multianode photomultipliers on each end. The fiber detector setup can be seen in figure 2.

The time-of-flight walls ToFD (Time of Flight Detector) and ToFI (Time of Flight Inner detector) generate the trigger and measure the flight time and charge Z of the fragments. ToFD consists of two layers plastic scintillator bars each 27 mm wide, 5 mm thick and 1000 mm long read out by two single anode photomultipliers from each end. Several bars in the center are dismounted to let the unreacted beam pass. The gap in layer one is three bars wide while in the second layer, which is shifted by the width of half a bar, a gap-width of two bars is sufficient. Mounted in a light-tight housing the active area is roughly 1200x80 cm^2. ToFI consists of one layer with twelve 5 mm square scintillation bars covering the innermost bars of ToFD for higher granularity at high intensities. Six bars on each side of the unreacted beam path are mounted on x-drives to adjust the gap.

A SEETRAM (SEcondary Electron TRAnsmission Monitor) detector, a scintillator and an ionization chamber positioned behind the time-of-flight walls are used to quantify the beam at different intensities. This allows a careful calibration in the overlapping range whereby SEETRAM can measure the highest intensities.
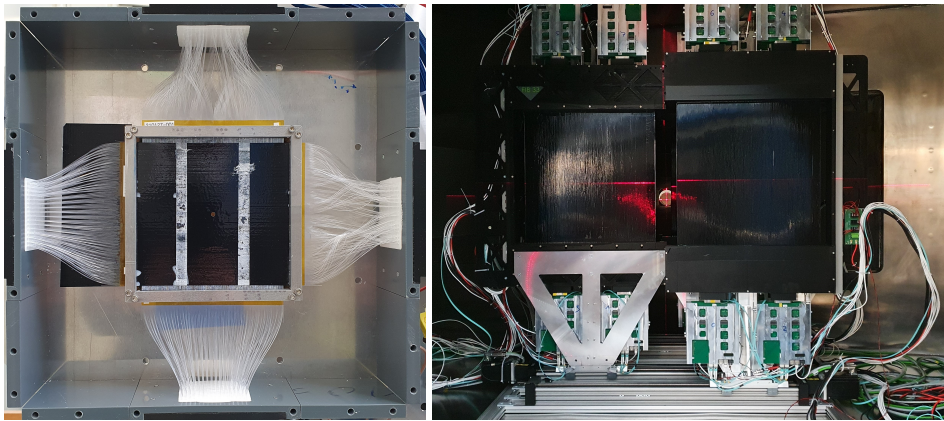
Figure 2. Fiber scintillator detectors for fragment tracking. Left: Two fiber detectors with 250 μm fibers, 10x10 cm^2 active area, and a 3 mm diameter hole, mounted in front of the magnet. Right: Four fiber detectors with 1000 μm fibers 50x50 cm^2 active area mounted inside the vacuum chamber behind GLAD. All detectors are mounted on drives to adjust the hole or gap.

2.2 The experimental campaign

The detection of all relevant fragments is of utmost importance. Therefore, prior to the experiment with ^{16}O beam, ^{4}He beam was taken in May 2021. Sweeping all detectors through the beam ensured careful threshold finding and calibration for particles with low Z. During the experiment in June/July 2021 with ^{16}O beam, the magnetic field was varied for a later reconstruction of the detector positions while tracking the well known momenta of unreacted ions. In total, we recorded 67 TB of data, where 89.6% of the runs were physics runs and the rest tuning and sweep runs. In table 1, the targets used and the corresponding measured hours are listed.

Unfortunately, in the tuning phase, it became clear that the accelerator could not provide the ^{16}O beam at 300 MeV/nucleon in a condition appropriate for the experiment. A switch to 500 MeV/nucleon improved the conditions, but limited the recorded statistics due to a lower number of virtual photons in the region of interest. In addition, beam focus and position were unstable. Therefore, we had to run with thinner targets at lower beam intensities and higher dead times of the data acquisition system than expected, which further reduced the recorded statistics.

Table 1. Targets, relative file size compared to recorded data of 67 TB and measured time. In total, we measured for 247 hours.

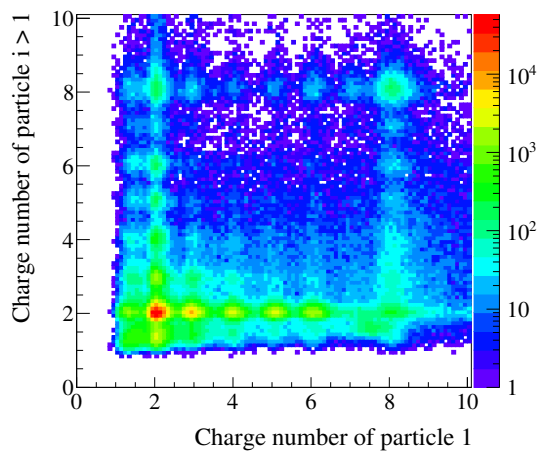| Target	Relative size in %	Measured time in h
Pb 38 μm	74.03	167.5
Pb 77 μm	6.39	17.3
C 252 μm	6.85	15.5
C 423 μm	2.85	5.4
Sn 104 μm	5.77	12.1
empty	2.36	22.1
other targets	1.75	7.2

3 Data analysis

Figure 3. Charge number of first particle measured by ToFD in one event vs. charge number of every other particle in this event.

Figure 3 shows the calibrated charge number of the first hit in ToFD in an event versus all other hits of this event. The Coulomb dissociation reaction products can be identified as (6,2) or (2,6). Other charges that are visible are a result of other reactions or pile-up of events. To identify matching pairs of the desired fragments, further cuts are necessary.
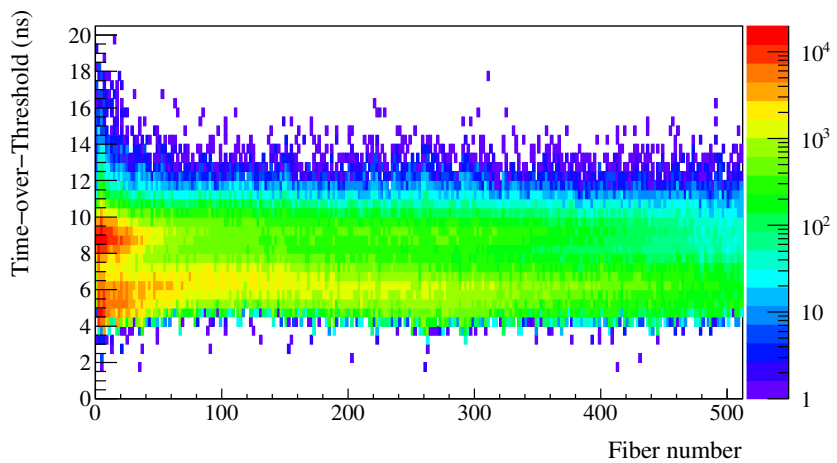
Figure 4. Fiber number of one detector behind GLAD vs. deposited energy as Time-over-Threshold. ^{12}C deposits more energy than ^{4}He, and they can be easily identified.

With time-of-flight cuts on the fiber detectors and selecting only matching pairs, we can separate ^{12}C and ^{4}He hits in the fiber detectors. In figure 4, the Time-over-Threshold for each

fiber of one large fiber detector is shown. ^{12}C deposits more energy than ^{4}He and the two can easily be separated. ^{4}He shows a larger angular distribution than ^{12}C.

We can use the well known momentum of the unreacted ^{16}O beam to calibrate our detector positions for tracking of the Coulomb dissociation reaction products. Using the information from all detectors we can then reconstruct the momentum of the reaction products at a common target point and hence the center-of-mass energy in figure 5. We normalize the tracked pairs to the number of incoming ^{16}O particles measured by SEETRAM, the number of atoms for the different targets used, the dead time, and a nuclear scaling factor. This scaling factor is necessary since the nuclear contribution measured with carbon target is dependent on the size of the target nuclei and thus needs to be rescaled for a lead target. By subtracting the nuclear breakup reaction we can then extract the Coulomb dissociation cross section.
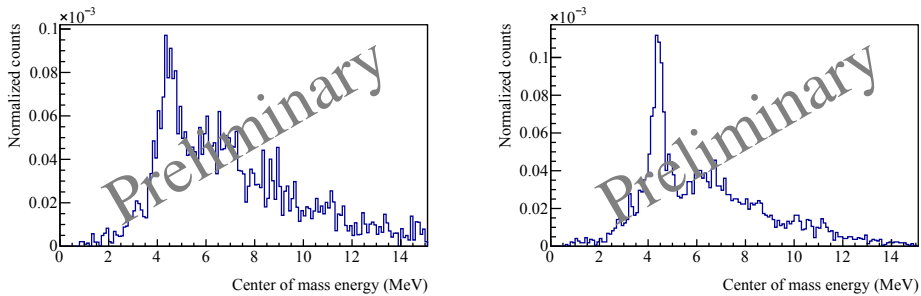

Figure 5. Counts of tracked ^{12}C and ^{4}He pairs as a function of the center-of-mass energy normalized to the number of incoming ^{16}O, number of target atoms, dead time, and a nuclear scaling factor. Left: Lead target, Right: Carbon target

The result is a very preliminary attempt in analyzing a small percentage of the recorded data and needs more careful calibration and tracking in the near future.

Acknowledgements

References

[1] R. deBoer, J. Görres, M. Wiescher, R. Azuma, A. Best, C. Brune, C. Fields, S. Jones, M. Pignatari, D. Sayre et al., Reviews of Modern Physics **89** (2017)

[2] M. Aliotta, R. Buompane, M. Couder, A. Couture, R.J. deBoer, A. Formicola, L. Gialanella, J. Glorius, G. Imbriani, M. Junker et al., Journal of Physics G: Nuclear and Particle Physics **49**, 010501 (2021)

[3] T. Sukhbold, S. Adams, Monthly Notices of the Royal Astronomical Society **492**, 2578 (2020)

[4] R. Farmer, M. Renzo, S.E. de Mink, P. Marchant, S. Justham, The Astrophysical Journal **887**, 53 (2019)

[5] R. Plag, R. Reifarth, M. Heil, F. Käppeler, G. Rupp, F. Voss, K. Wisshak, Phys. Rev. C **86**, 015805 (2012)

[6] R. Farmer, M. Renzo, S.E. de Mink, M. Fishbach, S. Justham, The Astrophysical Journal Letters **902**, L36 (2020)

[7] G. Baur, C. Bertulani, H. Rebel, Nuclear Physics A **458**, 188 (1986)

[8] C.A. Bertulani, Phys. Rev. C **49**, 2688 (1994)

[9] G. Baur, H. Rebel, Annual Review of Nuclear and Particle Science **46**, 321 (1996)

[10] C. Bertulani, A. Gade, Physics Reports **485**, 195 (2010)

[11] R. Reifarth, S. Altstadt, K. Göbel, T. Heftrich, M. Heil, A. Koloczek, C. Langer, R. Plag, M. Pohl, K. Sonnabend et al., Journal of Physics: Conference Series **665**, 012044 (2016)

[12] M. Heil, A. Kelić-Heil, L. Bott, T. Almusidi, H. Alvarez-Pol, L. Atar, L. Atkins, T. Aumann, J. Benlliure, K. Boretzky et al., The European physical journal / A **58**, 248 (2022)